Molecular Pharmacology Fast Forward. Published on December 28, 2018 as DOI: 10.1124/mol.118.114025
This article has not been copyedited and formatted. The final version may differ from this version.

Title Page

Title:

Mexiletine Block of Voltage-Gated Sodium Channels: Isoform- and State-Dependent Drug-Pore Interactions

Authors:

Hiroki Nakagawa

Tatsuo Munakata

Akihiko Sunami

Affiliation:

Department of Pharmaceutical Sciences, International University of Health and Welfare, Tochigi, Japan

Molecular Pharmacology Fast Forward. Published on December 28, 2018 as DOI: 10.1124/mol.118.114025
This article has not been copyedited and formatted. The final version may differ from this version.

Running Title Page

Running title: Isoform Differences in Mexiletine Block of Sodium Channels

Corresponding Author:

Akihiko Sunami

Address: Department of Pharmaceutical Sciences, International University of Health and Welfare, 2600-1 Kitakanemaru, Ohtawara, Tochigi 324-8501, Japan

Tel: +81-287-24-3517

Fax: +81-287-24-3521

Email: asunami@iuhw.ac.jp

Number of text pages: 31

Number of tables: 1

Number of figures: 9

Number of references: 42

Number of words in Abstract: 229

Number of words in Introduction: 734

Number of words in Discussion: 1473

List of non-standard abbreviations

Na_v voltage-gated sodium channel

WT wild-type

Molecular Pharmacology Fast Forward. Published on December 28, 2018 as DOI: 10.1124/mol.118.114025
This article has not been copyedited and formatted. The final version may differ from this version.

Abstract

Mexiletine is a class Ib antiarrhythmic drug and is also used clinically to reduce or prevent myotonia. In addition, mexiletine has neuroprotective effects in models of brain ischemia. We compared state-dependent affinities of mexiletine for $Na_v1.2$, $Na_v1.4$ and $Na_v1.5$, and examined the effects of mutations of transmembrane segment S6 residues on mexiletine block of $Na_v1.5$. Three channel isoforms had similar affinities of mexiletine for the rested state, and $Na_v1.4$ and $Na_v1.5$ had similar affinities for the open and inactivated states, while $Na_v1.2$ had lower affinity for these states than $Na_v1.4$ and $Na_v1.5$. Mutational studies revealed that the largest affinity change was observed for an Ala substitution of Phe in domain IV S6. In our homology modeling based on the bacterial Na^+ channel, mexiletine changed its location and orientation in the pore depending on the state of the channel, irrespective of the channel isoform. Mexiletine occurred upper in the pore in the open state and lower in the closed state. High affinity binding of mexiletine in the open states of $Na_v1.4$ and $Na_v1.5$ was caused by a π-π interaction with Phe, whereas mexiletine was located away from Phe in the open state of $Na_v1.2$. These results provide crucial information on the mechanism of isoform differences in state-dependent block by local anesthetics and related drugs. Mexiletine at upper locations in the open state may effectively cause an electrostatic mechanism of block.

Molecular Pharmacology Fast Forward. Published on December 28, 2018 as DOI: 10.1124/mol.118.114025
This article has not been copyedited and formatted. The final version may differ from this version.

Introduction

Mexiletine is a class Ib antiarrhythmic drug and is also considered as the first line for treating myotonic syndromes (Jackson et al., 1994; Hudson et al., 1995; Camerino et al., 2007). In addition, mexiletine is clinically useful to relieve neuropathic pain (Chabal et al., 1992) and protects brain neurons from injury in the models of ischemia (Stys and Lesiuk, 1996).

Mexiletine is an analogue of the local anesthetic lidocaine and exerts its therapeutic action through blockade of voltage-gated Na^+ channels. Although mexiletine blocks various channel isoforms, there are few reports on isoform differences in affinities of mexiletine. Affinity is known to vary as a function of the sodium channel gating state. It has been previously reported that affinity of mexiletine for the inactivated channel is 2-fold higher in $Na_v1.5$ than in $Na_v1.2$ (Weiser et al., 1999) and $Na_v1.5$ is more sensitive to use-dependent block by mexiletine than $Na_v1.7$ (Wang et al., 2015). On the other hand, mexiletine caused more block for $Na_v1.5$ than $Na_v1.2$ or $Na_v1.4$ by increasing the proportion of inactivated channels in $Na_v1.5$ (Kawagoe et al., 2002). Although isoform differences in local anesthetic affinity seem to be less than in toxin affinity (Fozzard and Hanck, 1996), understanding molecular mechanisms of isoform differences in affinities may contribute to rational design of isoform-selective and safer Na^+ channel blockers.

Elucidating the mechanisms of state-dependent block by local anesthetics is obviously important. Phe in domain IV S6 has long been known as a critical determinant of local anesthetic block (Ragsdale et al., 1994; Ragsdale et al., 1996). Other residues in S6 segments

of domains I, III and IV also affect the local anesthetic binding (Wang et al., 1998; Nau et al., 1999; Wang et al., 2000; Yarov-Yarovoy et al., 2001; Yarov-Yarovoy et al., 2002). Although mutations of these residues are well known to have different effects on the block of the closed, open and inactivated channels (Ragsdale et al., 1994; Ragsdale et al., 1996; Wang et al., 1998; Nau et al., 1999; Wang et al., 2000; Yarov-Yarovoy et al., 2001; Yarov-Yarovoy et al., 2002), the molecular mechanisms of these differences have not been clarified. Several structural models of Na^+ channels analyzed the interactions of local anesthetics with the pore residues in the closed (Tikhonov et al., 2006; Bruhova et al., 2008; Tikhonov and Zhorov, 2012) and open states (Lipkind and Fozzard, 2005; Tikhonov et al., 2006; Tikhonov and Zhorov, 2007; Tikhonov and Zhorov, 2017). Lidocaine molecules adopted different locations and orientations in the closed and open states of the $Na_v1.5$ model (Tikhonov et al., 2006), but most of their models are for either closed or open state, and for either channel isoform of $Na_v1.4$ or $Na_v1.5$.

To our knowledge, there is no comparison of local anesthetics docking into two or more different channel isoforms. Previously, homology models were based on the bacterial K^+ channel templates instead of the Na^+ channel templates (Lipkind and Fozzard, 2005; Tikhonov et al., 2006; Tikhonov and Zhorov, 2007; Bruhova et al., 2008). Nevertheless, sequences of mammalian Na^+ channels are more similar to the bacterial Na^+ channels than to the bacterial K^+ channels, and the Na^+ channel alignment is much less ambiguous than that of K^+ channels (Tikhonov and Zhorov, 2017). Actually, a novel distinct binding mode of lidocaine was found

Molecular Pharmacology Fast Forward. Published on December 28, 2018 as DOI: 10.1124/mol.118.114025
This article has not been copyedited and formatted. The final version may differ from this version.

in the Na^+ channel model based on the Na^+ channel template (Tikhonov and Zhorov, 2017), but this mode was not revealed in the models based on the K^+ channel templates (Tikhonov et al., 2006; Tikhonov and Zhorov, 2007).

In the present study, we addressed isoform differences in state-dependent block of mexiletine. First, we measured state-dependent affinities of mexiletine for $Na_v1.2$, $Na_v1.4$ and $Na_v1.5$. Affinities of mexiletine for the rested state were not different among these isoforms. $Na_v1.4$ and $Na_v1.5$ had similar affinities for the open and inactivated states, while $Na_v1.2$ had lower affinity for these states than $Na_v1.4$ and $Na_v1.5$. We next visualized the interactions of mexiletine with the pore residues using bacterial Na^+ channel templates. Mexiletine was located at a different place in the closed and open states irrespective of the channel isoform, and mexiletine was found closer to the extracellular space in the open state. High affinity binding of mexiletine in the open states of $Na_v1.4$ and $Na_v1.5$ was caused by a π-π interaction with Phe, which was consistent with our mutational studies of $Na_v1.5$. In contrast, mexiletine was not close to Phe in the open state of $Na_v1.2$.

Molecular Pharmacology Fast Forward. Published on December 28, 2018 as DOI: 10.1124/mol.118.114025
This article has not been copyedited and formatted. The final version may differ from this version.

Materials and Methods

Site-Directed Mutagenesis and Transfection Procedure. The human heart Na^+ channel α-subunit ($Na_v1.5$) clone in the pcDNA3.1$^+$ plasmid (Invitrogen, Carlsbad, CA) was a generous gift from Dr. N. Makita (Nagasaki University). All mutations (N406A, L1462A, L1462F, L1462E, F1760A) of $Na_v1.5$ were introduced using the QuikChange Site-Directed Mutagenesis Kit (Stratagene, La Jolla, CA), according to the manufacturer's protocols and as described in our previous report (Sunami et al., 2004). Mutations were confirmed by DNA sequencing of the full-length plasmid. Human embryonic kidney cells (HEK293 cells) were transiently transfected with the plasmid encoding wild-type (WT) or mutant $Na_v1.5$ channels using SuperFect (Qiagen, Hilden, Germany) in combination with a plasmid encoding CD8 (pIRES-CD8) to identify transfected cells with Dynabeads M-450 CD8 (Dynal, Oslo, Norway). Electrophysiological measurements were performed 24-72 h after transfection.

WT channels of the rat brain IIA ($Na_v1.2$) and the rat skeletal muscle Na^+ channel α-subunit ($Na_v1.4$) were stably expressed in HEK293 cells. The pRc/CMV plasmid (Invitrogen) encoding $Na_v1.2$ and the pCI-neo plasmid (Promega, Madison, WI) encoding $Na_v1.4$ were generous gifts from Dr. H. A. Fozzard (University of Chicago). Selection of stablely transfected cells was made in Dulbecco's modified Eagle's medium (DMEM) containing 600 μg/mL G418. The Na^+ channel β-subunits were not used in all experiments.

Molecular Pharmacology Fast Forward. Published on December 28, 2018 as DOI: 10.1124/mol.118.114025
This article has not been copyedited and formatted. The final version may differ from this version.

Electrophysiology and Data Analyses. Na^+ currents were recorded with the whole-cell configuration of patch clamp using an Axopatch 200B amplifier (Axon Instruments, Union City, CA). Currents were filtered at 5 kHz through a 4-pole Bessel filter and digitized at 100 kHz at 16-bit resolution with a Digidata 1322A acquisition system using pCLAMP 9 software (Axon Instruments). Pipettes had resistances between 1.0 and 1.5 MΩ. Recordings were made at room temperature (20-22°C) in a bathing solution containing (mM): 140 NaCl, 2.5 KCl, 2 $CaCl_2$, 1 $MgCl_2$, 10 HEPES (pH7.4 with NaOH). The pipette solution was (mM): 100 CsF, 40 NaCl, 10 HEPES (pH7.2 with CsOH).

To determine the activation parameters, the current-voltage (I-V) relationship was fitted to a transform of a Boltzmann distribution: $I = (V - V_{rev})G_{max} / \{1 + \exp[(V_{1/2} - V)/s]\}$, where I is the peak Na^+ current during the test pulse of voltage, V. The parameters estimated by the fitting were $V_{1/2}$ (the voltage for half-activation), s (slope factor), V_{rev} (the reversal potential), and G_{max} (the maximum peak conductance). After induction of steady-state inactivation by 1-s depolarizing prepulses from a holding potential of -130 mV, Na^+ currents were measured during test pulses to -20 or 0 mV applied every 4 s. Availability was described by the following Boltzmann equation: $I/I_{max} = 1/\{1 + \exp[(V - V_{1/2})/s]\}$, where I is the peak current, I_{max} is the maximum peak current, V is the prepulse voltage, $V_{1/2}$ is the voltage for half-inactivation, and s is the slope factor. The recovery from inactivation induced by 10-ms depolarization to -10 mV was monitored and the time course of recovery was fitted by a single exponential. Time to decay

Molecular Pharmacology Fast Forward. Published on December 28, 2018 as DOI: 10.1124/mol.118.114025
This article has not been copyedited and formatted. The final version may differ from this version.

from 90 to 10% of the peak current at 0 mV was also measured.

For mexiletine block experiments, a train of 30 pulses with 5-ms or 200-ms duration was applied at 300-ms interpulse intervals in the absence or presence of mexiletine. To compare the sensitivity of three channel isoforms to mexiletine block, we used holding potentials of -120 mV for $Na_v1.2$ and $Na_v1.4$, and -130 mV for $Na_v1.5$, and test potentials of 0 mV for $Na_v1.2$ and $Na_v1.4$, and -20 mV for $Na_v1.5$. These voltages were chosen based on the gating data (Table 1), and the voltages minimized the gating effects on mexiletine block. In $Na_v1.5$ mutant channels, tonic (or rested) and use-dependent block by mexiletine were produced by a train of 30 pulses with 5-ms or 200-ms duration applied to 0 mV (N406A, L1462E), -5 mV (L1462A) or -20 mV (L1462F, F1760A) from a holding potential of -130 mV (N406A, L1462A, F1760A) or -140 mV (L1462E, L1462F). The dissociation constants of mexiletine for the rested (K_R), open (K_O) and inactivated (K_I) states of the channels were determined by the concentration-response curves for tonic block, and for total block (tonic block + use-dependent block) caused by 5-ms and 200-ms depolarizing pulses, respectively. Mexiletine was obtained from Sigma (St. Louis, MO).

Data were analyzed using pCLAMP 9 (Axon Instruments) and SigmaPlot (SPSS, Chicago, IL). Pooled data are presented as the mean ± SD. Statistical comparisons were made by using one- or two-way ANOVA.

Molecular Pharmacology Fast Forward. Published on December 28, 2018 as DOI: 10.1124/mol.118.114025
This article has not been copyedited and formatted. The final version may differ from this version.

Molecular Modelling and Docking. As with our previous study (Sunami et al., 2004), we built homology models of the closed and open pores of $Na_v1.2$, $Na_v1.4$, $Na_v1.5$ based on the crystal structures of bacterial voltage-gated Na^+ channels, Na_vAb (for closed channel; PDB accession code 3RVY; Payandeh et al., 2011) and Na_vMs (for open channel; PDB accession code 5HVX; Sula et al., 2017) using MODELLER v9.17 (Šali et al., 1993). Sequence alignments of the pore regions of Na_vAb, Na_vMs, $Na_v1.2$, $Na_v1.4$ and $Na_v1.5$ are given in Fig. 1. The geometry optimization and partial charge calculation of mexiletine was carried out using the PM6 method of MOPAC2009 (MOPAC2009). Docking mexiletine in these models was performed using the lamarckian genetic algorithm of AutoDock4.2.6 and AutoDockTools (Morris et al., 2009). Side chain flexibility was allowed during docking for the following S6 residues: S401, V405, I408, N927, L931, F934, S1458, T1461, L1462, F1465, F1760, V1764 and Y1767 in $Na_v1.5$, and the~~ir~~ equivalent residues in $Na_v1.2$ and $Na_v1.4$. The docking grid was composed of 28 x 28 x 31 points with a point spacing of 1 Å. Autodock was run using the default parameter set except "Number of GA Runs" set to 350. The docking results were visualized using Biovia Discovery Studio Visualizer (Discovery Studio Visualizer).

Molecular Pharmacology Fast Forward. Published on December 28, 2018 as DOI: 10.1124/mol.118.114025
This article has not been copyedited and formatted. The final version may differ from this version.

Results

Isoform Differences in Mexiletine Block. We first compared the sensitivity of $Na_v1.2$, $Na_v1.4$ and $Na_v1.5$ to tonic block (first-pulse block or rested block) by mexiletine, which was measured at the holding potential of -120 mV for $Na_v1.2$ and $Na_v1.4$, and -130 mV for $Na_v1.5$. In $Na_v1.5$, tonic block by 40 μM mexiletine was 9.5 ± 5.8% (n = 5) and was not significantly different from the tonic block of $Na_v1.2$ (4.5 ± 9.6%, n = 5) or $Na_v1.4$ (8.0 ± 2.5%, n = 5) (Fig. 2A and 2B).

We next compared use-dependent block by mexiletine in three channel isoforms. In the control, a train of 30 pulses with 5-ms or 200-ms pulse duration produced no discernible block in three isoforms. After application of 40 μM mexiletine, the three isoforms exhibited use-dependent block with 5-ms pulses ($Na_v1.2$, 8.1 ± 1.3%, n = 5; $Na_v1.4$, 13.5 ± 2.7%, n = 5; $Na_v1.5$, 15.2 ± 4.5%, n = 5), and use-dependent block became bigger with 200-ms pulses in all isoforms ($Na_v1.2$, 20.2 ± 2.2%, n = 5; $Na_v1.4$, 37.2 ± 2.2% n = 5, $Na_v1.5$, 38.9 ± 5.4%, n = 5). The amount of activated and inactivated channel block by mexiletine was consistent with the previous reports (Ono et al., 1994; Carmeliet et al., 1998; Sasaki et al., 2004). Comparing the amounts of use-dependent block with 5-ms or 200-ms pulses among these three isoforms, $Na_v1.4$ and $Na_v1.5$ showed similar sensitivity to use-dependent block, and $Na_v1.2$ showed significantly less sensitivity than $Na_v1.4$ or $Na_v1.5$ ($p < 0.05$ or $p < 0.001$) (Fig. 2C).

Comparing the dissociation constants of mexiletine for three states of $Na_v1.2$, $Na_v1.4$ and $Na_v1.5$, K_R values were not much different among these three isoforms ($Na_v1.2$, K_R = 323.2

Molecular Pharmacology Fast Forward. Published on December 28, 2018 as DOI: 10.1124/mol.118.114025
This article has not been copyedited and formatted. The final version may differ from this version.

± 126.7 μM, n = 8; $Na_v1.4$, K_R = 315.1 ± 87.1 μM, n = 8; $Na_v1.5$, K_R = 270.3 ± 70.1 μM, n = 6) (Fig. 3). On the other hand, $Na_v1.4$ and $Na_v1.5$ showed similar affinities for the open and inactivated states and they had a 2-3-fold higher affinity for these states than $Na_v1.2$ ($Na_v1.2$, K_O = 190.5 ± 71.3 μM, n = 8, K_I = 163.6 ± 52.6 μM, n = 13; $Na_v1.4$, K_O = 95.2 ± 36.4 μM, n = 5, K_I = 50.9 ± 4.5 μM, n = 5; $Na_v1.5$, K_O = 92.4 ± 25.9 μM, n = 5, K_I = 48.3 ± 14.9 μM, n = 6). In the three channel isoforms, the open state affinity was 1.7-3.3-fold higher and the inactivated state affinity was 2.0-6.2-fold higher than the rested state.

Mutational Effects of S6 on Mexiletine Block. Because mutations of S6 residues, Asn in domain I (N418 in $Na_v1.2$, N434 in $Na_v1.4$), Leu in domain III (L1465 in $Na_v1.2$, L1280 in $Na_v1.4$) and Phe in domain IV (F1764 in $Na_v1.2$, F1579 in $Na_v1.4$) affected local anesthetic binding (Ragsdale et al., 1994; Ragsdale et al., 1996; Wang et al., 1998; Nau et al., 1999; Wang et al., 2000; Yarov-Yarovoy et al., 2001; Yarov-Yarovoy et al., 2002) and because most of these observations were from $Na_v1.2$ and $Na_v1.4$, we examined the effects of mutations of these equivalent residues (N406, L1462, F1760) on mexiletine block in $Na_v1.5$. Substitution of Asn-406 with Ala (N406A) significantly increased tonic block (26.7 ± 3.7%, n = 7, $p < 0.001$) and decreased use-dependent block by 40 μM mexiletine (12.5 ± 3.7%, n = 7, $p < 0.001$) compared to WT (tonic block, 9.5 ± 5.8%, n = 5; use-dependent block, 38.9 ± 5.4%, n = 5) (Fig. 4). Replacement of Phe-1760 with Ala (F1760A) reduced tonic block (0.0 ± 4.5%, n = 5) and

Molecular Pharmacology Fast Forward. Published on December 28, 2018 as DOI: 10.1124/mol.118.114025
This article has not been copyedited and formatted. The final version may differ from this version.

significantly decreased use-dependent block (3.2 ± 1.1%, n = 5, $p < 0.001$ vs. WT). Substitution of Leu-1462 with a negatively charged residue, Glu (L1462E) significantly decreased use-dependent block (11.4 ± 4.0%, n = 7, $p < 0.001$ vs. WT) and the Phe mutant of Leu-1462 (L1462F) significantly increased use-dependent block (49.1 ± 5.6%, n = 7, $p < 0.01$ vs. WT).

In Fig. 5, mutational effects of N406, L1462 and F1760 on the dissociation constants of mexiletine for three states were summarized. The largest affinity changes were observed in F1760A. F1760A decreased affinity of mexiletine for the inactivated state 9-fold (K_I = 429.5 ± 147.9 μM, n = 6). This was consistent with the previous reports showing that an important part of the local anesthetic binding site includes F1764 in $Na_v1.2$ (equivalent to F1760 in $Na_v1.5$) (Ragsdale et al., 1994; Ragsdale et al., 1996). In addition, F1760A decreased affinities for the rested and open states by 2-fold and 5-fold, respectively (K_R = 515.3 ± 183.6 μM, n = 5; K_O = 480.5 ± 138.4 μM, n = 6).

Changes in affinities for the open and inactivated states were also observed in L1462 mutations. L1462E decreased affinity for the open state 1.5-fold (K_O = 138.6 ± 22.8 μM, n = 5) and inactivated state 2.3-fold (K_I = 113.1 ± 25.0 μM, n = 5). L1462F increased affinities for the open and inactivated states by 1.8-fold and 2.3-fold, respectively (K_O = 51.3 ± 13.0 μM, n = 7; K_I = 21.3 ± 9.3 μM, n = 7), but L1462F had no effect on affinity for the rested state (K_R = 270.8 ± 77.4 μM, n = 6). In contrast, N406A increased affinity for the rested state by 2.7-fold (K_R = 101.3 ± 9.6 μM, n = 5) and decreased affinity for the inactivated state by 1.7-fold (K_I = 80.4 ±

9.4 μM, n = 5).

The Pore Models of Closed and Open $Na_v1.5$ Channel. We built homology models of the inner pore of the closed and open $Na_v1.5$ channel based on the crystal structures of bacterial voltage-gated Na^+ channels, Na_vAb (for closed channel) (Payandeh et al., 2011) and Na_vMs (for open channel) (Sula et al., 2017). Since the transmembrane pore regions of Na_vAb and Na_vMs have high sequence identities (McCusker et al., 2012), structure differences seen in the models are likely to be state-dependent rather than a consequence of sequence dissimilarities (Bagnéris et al., 2015). Our pore model was composed of P1 and P2 helices, non-helix linkers including the selectivity filter residues between the P1 and P2 helices, and the S6 segments (Fig. 6). In our pore model of $Na_v1.5$, F1760 in domain IV S6 and L1462 in domain III S6 faced the inner pore in both the closed and open states of the channel, which was consistent with the previous experimental evidence using a cysteine mutant of F1579 in $Na_v1.4$ (equivalent to F1760 in $Na_v1.5$) and the charged methanethiosulfonate (MTS) reagents (Sunami et al., 2004), and many studies of local anesthetic block (Ragsdale et al., 1994; Ragsdale et al., 1996; Wang et al., 2000; Yarov-Yarovoy et al., 2001; Nau et al., 2003). On the other hand, N406 in domain I S6 did not face the inner pore irrespective of the channel states.

Docking Simulations of Mexiletine in the Inner Pore of $Na_v1.5$. We docked mexiletine in

Molecular Pharmacology Fast Forward. Published on December 28, 2018 as DOI: 10.1124/mol.118.114025
This article has not been copyedited and formatted. The final version may differ from this version.

our inner pore model of the closed and open $Na_v1.5$ channels. The lowest energy poses of mexiletine docked inside the inner pore are shown in the closed and open channels (Fig. 7). In the closed channel, mexiletine was in the middle part of the inner pore, and the drug was not close to L1462 and F1760 (Fig. 7A). In the open channel, mexiletine moved closer to the extracellular space in the inner pore and was nearer to L1462 and F1760 compared to the closed channel (Fig. 7B). In particular, mexiletine interacted with F1760 through a π-π interaction with a distance of 3.65 Å between the aromatic ring centers of the drug and F1760. These docking results were consistent with those of the present mutational studies showing that F1760 was more involved in mexiletine binding in the open and inactivated channels than in the rested channel.

Docking Simulations of Mexiletine in the Inner Pore of $Na_v1.2$ and $Na_v1.4$. In the open and inactivated channels, $Na_v1.4$ had similar affinity for mexiletine compared to $Na_v1.5$, and $Na_v1.2$ had lower affinity than $Na_v1.4$ and $Na_v1.5$. In the rested channels, affinities for mexiletine were not different among these isoforms. To compare the relative location of mexiletine in these isoforms, we built the models of the inner pore of $Na_v1.2$ and $Na_v1.4$ in a similar manner to that of $Na_v1.5$, and then docked mexiletine inside the pore of the closed and open channels. In the closed $Na_v1.2$ channel, mexiletine was located relatively close to L1465 and away from F1764 (Fig. 8A). In the open $Na_v1.2$ channel, mexiletine moved toward the extracellular space in the

Molecular Pharmacology Fast Forward. Published on December 28, 2018 as DOI: 10.1124/mol.118.114025
This article has not been copyedited and formatted. The final version may differ from this version.

pore, but remained away from F1764 (Fig. 8B). On the other hand, mexiletine in $Na_v1.4$ behaved in a similar way to that in $Na_v1.5$. That is, mexiletine was located away from L1280 and F1579 in the closed $Na_v1.4$ channel, but mexiletine moved closer to F1760. The drug interacted with F1760 through a π-π interaction with a distance of 4.30 Å between the aromatic ring centers of the drug and F1760 in the open $Na_v1.4$ channel (Fig. 8C, D). These results suggest that the interaction between mexiletine and the pore residues depends on the channel isoforms and the states of the channel, and high affinity binding of mexiletine in the open states of $Na_v1.4$ and $Na_v1.5$ is caused by a π-π interaction with Phe.

Docking Simulations of Mexiletine in the Inner Pore of the Open $Na_v1.5$ Mutant Channels.

In the present mutational studies of $Na_v1.5$, F1760A and L1462E decreased affinities of mexiletine for the open and inactivated states. In contrast, L1462F increased drug affinities for the open and inactivated states. To examine the relative location of mexiletine in these mutant channels, we docked mexiletine inside the inner pore of the open mutant channels. In the open F1760A channel, mexiletine was located far away from A1760 and specific interactions between mexiletine and A1760 were not observed (Fig. 9A), which resulted in decreased affinities of mexiletine for the channel. In the open L1462E channel, mexiletine moved away from F1760 and interacted with E1462 through a salt bridge or hydrogen bonds (Fig. 9B). A salt bridge was formed between the positively-charged tertiary amino group of mexiletine and

Molecular Pharmacology Fast Forward. Published on December 28, 2018 as DOI: 10.1124/mol.118.114025
This article has not been copyedited and formatted. The final version may differ from this version.

the negatively-charged carboxyl group of E1462 (Fig. 9B), and hydrogen bonds were formed between two amino group hydrogens of mexiletine and the hydroxyl oxygen of E1462 (data not shown). Despite of the specific interaction of mexiletine with E1462, the observation that L1462E decreased mexiletine block suggests that the interaction between mexiletine and E1462 was not important in drug block and instead, less interaction of mexiletine with F1760 appeared to decrease mexiletine block. On the other hand, in the open L1462F channel, mexiletine was sandwiched between F1760 and a newly substituted residue, Phe at 1462 (Fig. 9C). Mexiletine interacted with F1760 through a T-shaped π-π interaction with a distance of 3.40 Å and with F1462 through a π-π interaction with a distance of 4.01 Å. Increased affinities of mexiletine caused by L1462F appeared to be due to π-π interactions between the aromatic rings of mexiletine and two phenylalanine residues. These results further support the idea that a π-π interaction of mexiletine with aromatic residues in the pore is crucial for high affinity binding of mexiletine to the open channel of $Na_v1.5$.

Molecular Pharmacology Fast Forward. Published on December 28, 2018 as DOI: 10.1124/mol.118.114025
This article has not been copyedited and formatted. The final version may differ from this version.

Discussion

The class Ib antiarrhythmic drug, mexiletine is used clinically to reduce or prevent myotonia (Jackson et al., 1994; Hudson et al., 1995) and has neuroprotective effects in models of brain ischemia (Stys and Lesiuk, 1996). In order to use the drug effectively for heart, muscle or neurons, the isoform-selectivity of channel block must be taken into account. Therefore, we identified and compared state-dependent affinities of mexiletine for three channel isoforms under the same experimental conditions.

The rested state affinities were not different among these three isoforms. $Na_v1.4$ and $Na_v1.5$ exhibited similar affinities for the open and inactivated states, which likely contributes to the therapeutic effects of mexiletine on myotonia as well as on cardiac arrhythmia. $Na_v1.2$ had a 2-3-fold lower affinity for these states than did $Na_v1.4$ and $Na_v1.5$, which was consistent with the previous report showing that affinity of mexiletine for the inactivated channel was 2-fold higher in $Na_v1.5$ than in $Na_v1.2$ (Weiser et al., 1999).

The rested and inactivated state affinities of $Na_v1.4$ obtained here were consistent with the previous study (Wang et al., 2004). The rested state affinity for $Na_v1.5$ was also in good agreement with the previous report (Weiser et al., 1999). In contrast, there were big differences in open state affinities between our data and the previous data (Wang et al., 1997; Wang et al., 2004). They directly measured the open state affinity from the mutant channels of $Na_v1.4$ or $Na_v1.5$ showing the late openings (IC_{50} of about 3 μM). Since the wild type channels of the

three isoforms have no or little persistent late currents under normal conditions, we estimated the open state affinity from the total block caused by a train of 30 pulses with 5-ms duration applied at 300-ms interpulse intervals. Consequently, the open state affinities in $Na_v1.4$ and $Na_v1.5$ were approximately 30-45-fold lower than those in the mutant channels (Wang et al., 1997; Wang et al., 2004). More pulses with higher frequency of stimulation may explain the experimental differences between their reports and our experiments. Nonetheless, our estimation of the open state affinity seems unlikely to alter the observation that $Na_v1.2$ has lower affinity for the open state than $Na_v1.4$ and $Na_v1.5$.

In our mutational studies of $Na_v1.5$, N406A increased affinity of mexiletine for the rested state and decreased affinity for the inactivated state, which was similar to the previous studies of etidocaine and bupivacaine exposed to the equivalent mutations of $Na_v1.2$ and $Na_v1.4$ (Nau et al., 1999; Yarov-Yarovoy et al., 2002). L1462E and L1462F decreased and increased affinities of mexiletine for the open and inactivated states, respectively. These findings were similar to the previous studies of bupivacaine using the equivalent mutations of $Na_v1.4$ (Nau et al., 2003). In our mutational studies, the biggest impact on mexiletine block was observed in F1760A. F1760A decreased affinities for the rested, open and inactivated states 2-fold, 5-fold and 9-fold, respectively, which resembled the results of the previous study of mexiletine in rat $Na_v1.5$ (Weiser et al., 1999).

In our model of $Na_v1.5$, L1462 and F1760 faced the inner pore, and N406 faced away

Molecular Pharmacology Fast Forward. Published on December 28, 2018 as DOI: 10.1124/mol.118.114025
This article has not been copyedited and formatted. The final version may differ from this version.

from the pore, irrespective of the channel states. Consistent with our model, the KcsA-based model of the closed $Na_v1.5$ channel indicated that Asp does not face the pore (Bruhova et al., 2008). Although N406A changed affinities of mexiletine for the rested and inactivated states, this affinity change seems to be mediated by allosteric influences.

In our docking, mexiletine was located differently depending on the state. In the closed states of $Na_v1.4$ and $Na_v1.5$, mexiletine was not close to or was located away from Phe. Once $Na_v1.4$ and $Na_v1.5$ channels opened, mexiletine approached Phe and formed π-π interactions. Consistent with this, F1760A decreased affinity of mexiletine more markedly for the open state than for the rested state, suggesting that F1760 is more involved in mexiletine block in the open state than in the closed state. In addition, it is noteworthy that mexiletine is a potent open channel blocker of $Na_v1.4$ and $Na_v1.5$ (Wang et al., 1997; Wang et al., 2004).

In contrast, in the $Na_v1.2$ model, mexiletine was located away from Phe even in the open state. The simplest interpretation of these results is that mexiletine has no or little interaction with Phe in the open state of $Na_v1.2$. To our knowledge, there is no evidence that mexiletine directly interacts with the open state of $Na_v1.2$. In addition, our estimation of the open state affinity of mexiletine showed that $Na_v1.2$ has a 2-fold lower affinity for the open state than $Na_v1.4$ and $Na_v1.5$. These results indicated that Phe is not a key residue for mexiletine block in the open state of $Na_v1.2$. Consistent with this, Phe was also less important to mexiletine block in the rested and inactivated states of $Na_v1.2$ than to binding of the drug to $Na_v1.5$ (Weiser

Molecular Pharmacology Fast Forward. Published on December 28, 2018 as DOI: 10.1124/mol.118.114025
This article has not been copyedited and formatted. The final version may differ from this version.

et al., 1999). Instead, another key aromatic residue, Tyr contributed more importantly to mexiletine block in the inactivated state of $Na_v1.2$.

The previous studies using unnatural fluorinated phenylalanine derivatives demonstrated that $Na_v1.4$ and $Na_v1.5$ channels form cation-π interactions with lidocaine and mexiletine at Phe and produce use-dependent block (Ahern et al., 2008; Pless et al., 2011). A cation-π interaction likely occurs in the inactivated state because class Ib antiarrhythmic drugs including lidocaine and mexiletine having higher affinities for the inactivated state produce use-dependent block through a cation-π interaction, but class Ia and Ic drugs including quinidine and flecainide prefer the open channel and rely less on this interaction (Pless et al., 2011). Since mexiletine seems to change its position and orientation depending on the channel state, it is possible that mexiletine binds to Phe through a π-π interaction in the open state and through a cation-π interaction in the inactivated state. Structural models of the inactivated state are not yet available to confirm this hypothesis since prokaryotic Na^+ channels have no fast inactivation (Pavlov et al., 2005) and the electrophysiological states of electric eel Na^+ channels with fast inactivation of which structures were recently reported are yet to be defined (Yan et al., 2017).

Our models agree with the following experimental data. 1) Mutations of L1462 and F1760 affect mexiletine block, and L1462 and F1760 face the pore in the model. 2) $Na_v1.4$ and $Na_v1.5$ have similar affinities for the closed and open states, and the relative locations of mexiletine are similar in the models of closed and open states of $Na_v1.4$ and $Na_v1.5$. 3) $Na_v1.2$

Molecular Pharmacology Fast Forward. Published on December 28, 2018 as DOI: 10.1124/mol.118.114025
This article has not been copyedited and formatted. The final version may differ from this version.

has lower affinity for the open state than $Na_v1.4$ and $Na_v1.5$, and the relative location of mexiletine in the model of open $Na_v1.2$ is different from those of open $Na_v1.4$ and $Na_v1.5$. 4) Decrease in affinity mediated by F1760A is more marked in the open state than in the closed state, and mexiletine interacts with F1760 through a π-π interaction in the model of open $Na_v1.5$ and is not close to F1760 in the model of closed $Na_v1.5$. 5) F1760A decreases affinity for the open state 5-fold (-1.0 kcal/mol) and mexiletine is located far away from A1760 in the model of the open channel containing F1760A.

In several previous models, local anesthetics adopt a horizontal orientation with respect to the ion permeation pathway in the closed channel and a vertical orientation in the open channel (Lipkind and Fozzard, 2005; Tikhonov et al., 2006; Tikhonov and Zhorov., 2007; Bruhova et al., 2008; Tikhonov and Zhorov., 2012). On the other hand, several local anesthetics adopt horizontal, vertical and intermediate (angular) orientations in the closed channel (Bruhova et al., 2008), and horizontal and two distinct vertical orientations in the open channel (Tikhonov and Zhorov., 2017). In our docking, mexiletine appeared not to adopt either horizontal or vertical orientations in any state. Differences in ligand orientations among the models might be, in part, because of different channel templates used, different channel states and different channel isoforms.

In our model, mexiletine occurred closer to the extracellular space in the open channel regardless of the channel isoform. This may facilitate the electrostatic mechanism of block

Molecular Pharmacology Fast Forward. Published on December 28, 2018 as DOI: 10.1124/mol.118.114025
This article has not been copyedited and formatted. The final version may differ from this version.

(Lipkind and Fozzard, 2005; Tikhonov et al., 2006; McNulty et al., 2007) and explain a greater block in the open channel. Specific binding of the aromatic ring of mexiletine to Phe likely helps locate the ammonium group upward in $Na_v1.4$ and $Na_v1.5$. In addition, our docking and experimental results suggest that the amino acid residues lining the pore, which are common to $Na_v1.4$ and $Na_v1.5$, but not common to $Na_v1.2$ (Fig. 1) may help mexiletine form a π-π interaction with Phe in the open states. Consequently, mexiletine may work better in $Na_v1.4$ or $Na_v1.5$ than $Na_v1.2$. Further experimental studies are needed to test this hypothesis.

In conclusion, $Na_v1.4$ and $Na_v1.5$ had similar affinities and interactions for mexiletine. This may explain the therapeutic effects of mexiletine on myotonia as well as on cardiac arrhythmia. Visualization of isoform differences in state-dependent block may contribute to rational design of isoform-selective and safer drugs.

Molecular Pharmacology Fast Forward. Published on December 28, 2018 as DOI: 10.1124/mol.118.114025
This article has not been copyedited and formatted. The final version may differ from this version.

Acknowledgments

We are indebted to Dr. H. A. Fozzard for his support of this work and to Dr. S. C. Dudley for reading and commenting on the manuscript. Dr. N. Makita generously provided the $Na_v1.5$ clone. The technical assistance of N. Ishimaru is also appreciated.

Molecular Pharmacology Fast Forward. Published on December 28, 2018 as DOI: 10.1124/mol.118.114025
This article has not been copyedited and formatted. The final version may differ from this version.

Authorship Contributions

Participated in research design: Nakagawa, Munakata, Sunami

Conducted experiments: Nakagawa, Munakata, Sunami

Performed data analysis: Nakagawa, Munakata, Sunami

Wrote or contributed to the writing of the manuscript: Nakagawa, Munakata, Sunami

References

Ahern CA, Eastwood AL, Dougherty DA, Horn R (2008) Electrostatic contributions of aromatic residues in the local anesthetic receptor of voltage-gated sodium channels. *Circ Res* **102:**86-94.

Bagnéris C, Naylor CE, McCusker EC, Wallace BA (2015) Structural model of the open-closed-inactivated cycle of prokaryotic voltage-gated sodium channels. *J Gen Physiol* **145:**5-16.

Bruhova I, Tikhonov DB, Zhorov BS (2008) Access and binding of local anesthetics in the closed sodium channel. *Mol Pharmacol* **74:**1033-1045.

Camerino DC, Tricarico D, Desaphy JF (2007) Ion channel pharmacology. *Neurotherapeutics* **4:**184-198.

Carmeliet E, Mubagwa K (1998) Antiarrhythmic drugs and cardiac ion channels: mechanisms of action. *Prog Biophys Mol Biol* **70:**1-72.

Chabal C, Jacobson L, Mariano A, Chaney E, Britell CW (1992) The use of oral mexiletine for the treatment of pain after peripheral nerve injury. *Anesthesiology* **76:**513-517.

Discovery Studio Visualizer. Dassault Systemes Biovia. Discovery Studio Modeling Environment. San Diego, CA: Dassault Systèmes, 2016

Fozzard HA, Hanck DA (1996) Structure and function of voltage-dependent sodium channels: comparison of brain II and cardiac isoforms. *Physiol Rev* **76:**887-926.

Hudson AJ, Ebers GC, Bulman DE (1995) The skeletal muscle sodium and chloride channel

diseases. *Brain* **118(Pt 2):**547-563.

Jackson CE, Barohn RJ, Ptacek LJ (1994) Paramyotonia congenita: abnormal short exercise test, and improvement after mexiletine therapy. *Muscle Nerve* **17:**763-768.

Kawagoe H, Yamaoka K, Kinoshita E, Fujimoto Y, Maejima H, Yuki T, Seyama I (2002) Molecular basis for exaggerated sensitivity to mexiletine in the cardiac isoform of the fast Na channel. *FEBS Lett* **513:**235-41.

Lipkind GM, Fozzard HA (2005) Molecular modeling of local anesthetic drug binding by voltage-gated sodium channels. *Mol Pharmacol* **68:**1611-1622.

McCusker EC, Bagnéris C, Naylor CE, Cole AR, D'Avanzo N, Nichols CG, Wallace BA (2012) Structure of a bacterial voltage-gated sodium channel pore reveals mechanisms of opening and closing. *Nat Commun* **3:**1102.

McNulty MM, Edgerton GB, Shah RD, Hanck DA, Fozzard HA, Lipkind GM (2007) Charge at the lidocaine binding site residue Phe-1759 affects permeation in human cardiac voltage-gated sodium channels. *J Physiol* **581(Pt 2):**741-755.

MOPAC2009. James J. P. Stewart, Stewart Computational Chemistry, Colorado Springs, CO, USA, http://OpenMOPAC.net, 2008

Morris GM, Huey R, Lindstrom W, Sanner MF, Belew RK, Goodsell DS, Olson AJ (2009) AutoDock4 and AutoDockTools4: Automated docking with selective receptor flexibility. *J Comput Chem* **30:**2785-2791.

Nau C, Wang SY, Strichartz GR, Wang GK (1999) Point mutations at N434 in D1-S6 of mu1 Na^+ channels modulate binding affinity and stereoselectivity of local anesthetic enantiomers. *Mol Pharmacol* **56:**404-413.

Nau C, Wang SY, Wang GK (2003) Point mutations at L1280 in Nav1.4 channel D3-S6 modulate binding affinity and stereoselectivity of bupivacaine enantiomers. *Mol Pharmacol* **63:**1398-1406.

Ono M, Sunami A, Sawanobori T, Hiraoka M (1994) External pH modifies sodium channel block by mexiletine in guinea pig ventricular myocytes. *Cardiovasc Res* **28:**973-979.

Pavlov E, Bladen C, Winkfein R, Diao C, Dhaliwal P, French RJ (2005) The pore, not cytoplasmic domains, underlies inactivation in a prokaryotic sodium channel. *Biophys J.* **89:**232-42.

Payandeh J, Scheuer T, Zheng N, Catterall WA (2011) The crystal structure of a voltage-gated sodium channel. *Nature* **475:**353-358.

Pless SA, Galpin JD, Frankel A, Ahern CA (2011) Molecular basis for class Ib anti-arrhythmic inhibition of cardiac sodium channels. *Nat Commun* **2:**351.

Ragsdale DS, McPhee JC, Scheuer T, Catterall WA (1994) Molecular determinants of state-dependent block of Na^+ channels by local anesthetics. *Science* **265:**1724-1728.

Ragsdale DS, McPhee JC, Scheuer T, Catterall WA (1996) Common molecular determinants of local anesthetic, antiarrhythmic, and anticonvulsant block of voltage-gated Na^+ channels.

Proc Natl Acad Sci U S A **93:**9270-9275.

Šali A, Blundell TL (1993) Comparative protein modelling by satisfaction of spatial restraints. *J Mol Biol* **234:**779-815.

Sasaki K, Makita N, Sunami A, Sakurada H, Shirai N, Yokoi H, Kimura A, Tohse N, Hiraoka M, Kitabatake A (2004) Unexpected mexiletine responses of a mutant cardiac Na^+ channel implicate the selectivity filter as a structural determinant of antiarrhythmic drug access. *Mol Pharmacol* **66:**330-336.

Stys PK, Lesiuk H (1996) Correlation between electrophysiological effects of mexiletine and ischemic protection in central nervous system white matter. *Neuroscience* **71:**27-36.

Sula A, Booker J, Ng LC, Naylor CE, DeCaen PG, Wallace BA (2017) The complete structure of an activated open sodium channel. *Nat Commun* **8:**14205.

Sunami A, Tracey A, Glaaser IW, Lipkind GM, Hanck DA, Fozzard HA (2004) Accessibility of mid-segment domain IV S6 residues of the voltage-gated Na^+ channel to methanethiosulfonate reagents. *J Physiol* **561:**403-413.

Tikhonov DB, Bruhova I, Zhorov BS (2006) Atomic determinants of state-dependent block of sodium channels by charged local anesthetics and benzocaine. FEBS Lett **580:**6027-6032.

Tikhonov DB, Zhorov BS (2007) Sodium channels: ionic model of slow inactivation and state-dependent drug binding. *Biophys J* **93:**1557-1570.

Tikhonov DB, Zhorov BS (2012) Architecture and pore block of eukaryotic voltage-gated

sodium channels in view of NavAb bacterial sodium channel structure. *Mol Pharmacol* **82:**97-104.

Tikhonov DB, Zhorov BS (2017) Mechanism of sodium channel block by local anesthetics, antiarrhythmics, and anticonvulsants. *J Gen Physiol* **149:**465-481.

Wang DW, Yazawa K, Makita N, George AL Jr, Bennett PB (1997) Pharmacological targeting of long QT mutant sodium channels. *J Clin Invest* **99:**1714-1720.

Wang GK, Quan C, Wang SY (1998) Local anesthetic block of batrachotoxin-resistant muscle Na^+ channels. *Mol Pharmacol.* **54:**389-396.

Wang GK, Russell C, Wang SY (2004) Mexiletine block of wild-type and inactivation-deficient human skeletal muscle hNav1.4 Na^+ channels. *J Physiol* **554(Pt 3):**621-633.

Wang SY, Nau C, Wang GK (2000) Residues in Na^+ channel D3-S6 segment modulate both batrachotoxin and local anesthetic affinities. *Biophys J* **79:**1379-1387.

Wang Y, Mi J, Lu K, Lu Y, Wang K (2015) Comparison of gating properties and use-dependent block of Nav1.5 and Nav1.7 channels by anti-arrhythmics mexiletine and lidocaine. *PLoS One* **10:**e0128653.

Weiser T, Qu Y, Catterall WA, Scheuer T (1999) Differential interaction of R-mexiletine with the local anesthetic receptor site on brain and heart sodium channel alpha-subunits. *Mol Pharmacol* **56:**1238-1244.

Yan Z, Zhou Q, Wang L, Wu J, Zhao Y, Huang G, Peng W, Shen H, Lei J, Yan N (2017)

Structure of the $Na_v1.4$-β1 complex from electric eel. *Cell* **170:**470-482.

Yarov-Yarovoy V, Brown J, Sharp EM, Clare JJ, Scheuer T, Catterall WA (2001) Molecular determinants of voltage-dependent gating and binding of pore-blocking drugs in transmembrane segment IIIS6 of the Na^+ channel alpha subunit. *J Biol Chem* **276:**20-27.

Yarov-Yarovoy V, McPhee JC, Idsvoog D, Pate C, Scheuer T, Catterall WA (2002) Role of amino acid residues in transmembrane segments IS6 and IIS6 of the Na^+ channel alpha subunit in voltage-dependent gating and drug block. *J Biol Chem* **277:**35393-35401.

Molecular Pharmacology Fast Forward. Published on December 28, 2018 as DOI: 10.1124/mol.118.114025
This article has not been copyedited and formatted. The final version may differ from this version.

Footnotes

This work was partially supported by the grant from International University of Health and Welfare to Akihiko Sunami.

Molecular Pharmacology Fast Forward. Published on December 28, 2018 as DOI: 10.1124/mol.118.114025
This article has not been copyedited and formatted. The final version may differ from this version.

Legends for Figures

Fig. 1. Sequence alignment of the pore regions of Na_vAb, Na_vMs, $Na_v1.2$, $Na_v1.4$ and $Na_v1.5$. The proposed identities of the P1 and P2 helices, and the inner helix or the transmembrane segment S6 are indicated above the sequences. The number next to each inner helix or S6 sequence indicates the amino acid number of the end of each inner helix or S6. The amino acid residues indicated in bold are conserved among $Na_v1.2$, $Na_v1.4$ and $Na_v1.5$. The residues in red (N406, L1462, F1760) were mutated in the present study and these are conserved among these three channels.

Fig. 2. Tonic and use-dependent block by mexiletine of $Na_v1.2$, $Na_v1.4$ and $Na_v1.5$. A, typical current traces before (Con) and after application of 40 μM mexiletine (Mex) recorded from $Na_v1.2$ (left), $Na_v1.4$ (middle) and $Na_v1.5$ (right). To produce tonic block (TB) and use-dependent block (UDB) by mexiletine, a train of 30 pulses with 200-ms duration was applied at 300-ms interpulse intervals in the absence and presence of mexiletine. Current traces are during the 1st pulse for the control, and the 1st and 30th pulses for mexiletine. See Materials and Methods for the voltages of the pulse protocol. B, tonic block of $Na_v1.2$, $Na_v1.4$ and $Na_v1.5$ by 40 μM mexiletine. C, use-dependent block of $Na_v1.2$, $Na_v1.4$ and $Na_v1.5$ by 40 μM mexiletine. Use-dependent block by mexiletine was produced by 30 pulses with 5-ms (left) or 200-ms pulse duration (PD) (right) at 300-ms interpulse intervals. In B and C, data represent

Molecular Pharmacology Fast Forward. Published on December 28, 2018 as DOI: 10.1124/mol.118.114025
This article has not been copyedited and formatted. The final version may differ from this version.

the mean ± SD from five cells. *$p < 0.05$, ***$p < 0.001$ compared with $Na_v1.5$, +++ $p < 0.001$ compared with $Na_v1.4$, two-way ANOVA followed by Bonferroni test.

Fig. 3. Dissociation constants of mexiletine for three states of $Na_v1.2$, $Na_v1.4$ and $Na_v1.5$. The dissociation constants of mexiletine for the rested (K_R), open (K_O) and inactivated (K_I) states were determined by the concentration-response curves for tonic block, and for total block (tonic block + use-dependent block) caused by 5-ms and 200-ms depolarizing pulses, respectively. Data represent the mean ± SD from five to eight cells except $Na_v1.2$ K_I (thirteen cells). See Materials and Methods, and the inset shown in Fig. 2A for more details of definition of block and dissociation constants.

Fig. 4. Effects of $Na_v1.5$ mutants on mexiletine block. A, typical current traces before (Con) and after application of 40 μM mexiletine (Mex) recorded from $Na_v1.5$ wild-type (WT), N406A, L1462E and F1760A. Current traces in each panel are during the 1st pulse in a train of 30 pulses for the control, and the 1st and 30th pulses for mexiletine. B, summary of tonic block of WT, and mutants of N406, L1462 and F1760 by 40 μM mexiletine. C, summary of use-dependent block of WT, and mutants of N406, L1462 and F1760 by 40 μM mexiletine. In A through C, tonic and use-dependent block were produced by a train of 30 pulses with 200-ms duration applied at 300-ms interpulse intervals in the absence and presence of mexiletine. See Materials

Molecular Pharmacology Fast Forward. Published on December 28, 2018 as DOI: 10.1124/mol.118.114025
This article has not been copyedited and formatted. The final version may differ from this version.

and Methods for the voltages of the pulse protocol. In B and C, data represent the mean ± SD from five to seven cells. ***$p < 0.001$, **$p < 0.01$ compared with WT, one-way ANOVA followed by Dunnett test.

Fig. 5. Effects of $Na_v1.5$ mutants on dissociation constants of mexiletine for three states. Data represent the mean ± SD from five to eight cells. See Fig. 3 for definition of dissociation constants.

Fig. 6. The pore models of closed and open $Na_v1.5$ channels based on the structures of bacterial Na^+ channels, Na_vAb (for closed channel) and Na_vMs (for open channel). Panels A and C, and panels B and D are closed and open $Na_v1.5$ channels, respectively, and panels A and B are top views, and panels C and D are side views of those. Each pore model was composed of P1 and P2 helices, non-helix linkers including selectivity filter residues between P1 and P2 helices, and S6 segments. The linkers between P2 helices and S6 helices are also shown, but their location and arrangement are not necessarily based on the homology sequences of Na_vAb and Na_vMs. The closed and open channels are colored light pink and silver, respectively, and the helices and the linkers are shown as ribbons and rods, respectively. Residues N406 (red) in domain I S6 (DIS6), L1462 (green) in DIIIS6 and F1760 (blue) in DIVS6 are represented as sticks.

Molecular Pharmacology Fast Forward. Published on December 28, 2018 as DOI: 10.1124/mol.118.114025
This article has not been copyedited and formatted. The final version may differ from this version.

Fig. 7. Docking simulations of mexiletine inside the inner pore of the closed (A) and open $Na_v1.5$ channels (B). Side views of the lowest energy binding orientation of mexiletine (yellow stick) docked inside the inner pore are shown in the closed (A) and open channels (B). L1462 and F1760 are represented as green and blue sticks, respectively. The left-hand or right-hand inset in each panel is a magnified view showing the relative location of mexiletine to L1462 and F1760, where the distances between the aromatic ring centers of F1760 and mexiletine, and between the aromatic ring center of F1760 and the tertiary amino group of mexiletine are shown.

Fig. 8. Docking simulations of mexiletine inside the inner pore of $Na_v1.2$ and $Na_v1.4$. Side views of the lowest energy binding orientation of mexiletine (yellow stick) docked inside the inner pore are shown in the closed (A, C) and open channels (B, D) for $Na_v1.2$ (A, B) and $Na_v1.4$ (C, D). Colors and magnified views of the relative location of mexiletine to L1462 and F1760 are the same as described in the legend to Fig. 7.

Fig. 9. Detailed view of mexiletine binding in the open $Na_v1.5$ mutant channels. Side views of the lowest energy binding orientation of mexiletine (yellow stick) docked inside the inner pore are shown in the open channels of F1760A (A), L1462E (B) and L1462F (C). Domain II S6 is not depicted for clarity in each panel. Residues at 1760 (A1760, F1760) are shown as blue sticks, and residues at 1462 (L1462, E1462, F1462) are shown as green sticks. The distances between

Molecular Pharmacology Fast Forward. Published on December 28, 2018 as DOI: 10.1124/mol.118.114025
This article has not been copyedited and formatted. The final version may differ from this version.

F1760 and substituted residues (A1760, E1462, F1462), and the aromatic ring center and the tertiary amino group of mexiletine are depicted to examine whether these pore residues make specific interactions with the drug including π-π interaction, cation-π interaction, salt bridge and hydrogen bond.

Molecular Pharmacology Fast Forward. Published on December 28, 2018 as DOI: 10.1124/mol.118.114025
This article has not been copyedited and formatted. The final version may differ from this version.

Table 1 Gating parameters of $Na_v1.2$, $Na_v1.4$, $Na_v1.5$ and $Na_v1.5$ mutants

	Activation			Inactivation			I_{Na} decay (at 0 mV)		Recovery	
	$V_{1/2}$ (mV)	s (mV)	n	$V_{1/2}$ (mV)	s (mV)	n	Decay time (ms)	n	τ (ms)	n
$Na_v1.2$	-19.4 ± 3.4	5.6 ± 0.6	8	-54.1 ± 3.4	5.1 ± 0.8	8	1.3 ± 0.3	8	1.0 ± 0.3	7
$Na_v1.4$	-22.4 ± 2.5	6.4 ± 0.7	5	-60.3 ± 5.1	6.7 ± 0.7	6	1.0 ± 0.1	5	0.8 ± 0.2	5
$Na_v1.5$	-51.3 ± 5.8	5.6 ± 0.4	5	-90.3 ± 6.5	4.9 ± 0.6	8	1.8 ± 1.1	5	5.5 ± 0.7	6
$Na_v1.5$ mutants										
N406A	-34.0 ± 6.9	8.1 ± 1.7	6	-89.0 ± 3.7	5.0 ± 0.6	8	0.9 ± 0.2	6	1.4 ± 0.3	8
L1462A	-38.0 ± 2.7	6.4 ± 1.0	6	-92.4 ± 2.4	4.8 ± 0.7	6	0.7 ± 0.1	6	8.9 ± 1.2	6
L1462E	-31.8 ± 6.8	6.9 ± 0.8	4	-98.2 ± 4.9	5.7 ± 0.9	5	0.8 ± 0.2	4	11.6 ± 3.4	4
L1462F	-44.4 ± 4.9	6.0 ± 0.4	5	-101.0 ± 6.9	4.5 ± 0.7	12	0.5 ± 0.2	5	11.3 ± 4.5	7
F1760A	-52.3 ± 5.9	5.8 ± 0.7	6	-81.9 ± 6.0	4.8 ± 0.3	9	2.0 ± 1.0	6	4.4 ± 0.7	6

The voltage dependence of activation and inactivation, and recovery from fast inactivation were measured by the method described in "Materials and Methods". $V_{1/2}$: voltage for half-activation or half-inactivation, s: slope factor, n: number of cells, Decay time: time to decay from 90 to 10% of the peak current at 0 mV, τ: time constant. Data represent the mean ± SD.

Molecular Pharmacology Fast Forward. Published on December 28, 2018 as DOI: 10.1124/mol.118.114025
This article has not been copyedited and formatted. The final version may differ from this version.

	P1-helix		P2-helix		inner helix (S6)	
Na_vAb	GESFYTLFQVM	TLESW	SMGIVRPLMEV	YP	YAWVFFIPFIFVVTFVMINLVVAIIVDAM	221
Na_vMs	SKSLYTLFQVM	TLESW	SMGIVRPVMNV	HP	NAWVFFIPFIMLTTFTVLNLFIGIIVDAM	222
$Na_v1.2$ I	S**WAFL**S**LFRLM**	**TQD**F**W**	**-E**N**L**Y**Q**L**TLR**A	**AGK**	T**YMIFF**VLV**IFLGSFYL**I**NLILAVVAMAY**	428
$Na_v1.2$ II	**FH**S**FLI**V**FR**V**L**	**CGE-W**	**IETMWDCMEV**A	**GQ**T	M**CLTVF**MM**VMVIGNLVVLNLFLALLLSSF**	986
$Na_v1.2$ III	**G**L**GYL**S**LLQVA**	**TFKGW**	**-MDIMYAAVDS**	*	**YMY**L**YFVIFIIFGSFFTLNLFIGVIIDNF**	1476
$Na_v1.2$ IV	G**NS**MI**CLF**Q**IT**	**TSAGW**	**-DGLLAPILN**S	**	V**GIFFF**VS**YIIISFL**V**VVNMYIA**V**ILENF**	1779
$Na_v1.4$ I	S**WAFL**A**LFRLM**	**TQD**Y**W**	**-E**N**L**F**Q**L**TLR**A	**AGK**	T**YMIFF**VVI**IFLGSFYL**I**NLILAVVAMAY**	444
$Na_v1.4$ II	**FH**S**FLI**V**FR**I**L**	**CGE-W**	**IETMWDCMEV**A	**GQ**A	M**CLTVF**LM**VMVIGNLVVLNLFLALLLSSF**	799
$Na_v1.4$ III	**G**L**GYL**S**LLQVA**	**TFKGW**	**-MDIMYAAVDS**	#	**YMY**L**YFVIFIIFGSFFTLNLFIGVIIDNF**	1291
$Na_v1.4$ IV	G**NS**II**CLF**E**IT**	**TSAGW**	**-DGLLNPILN**S	##	I**GICFF**CS**YIIISFLIVVNMYIA**I**ILENF**	1594
$Na_v1.5$ I	A**WAFL**A**LFRLM**	**TQD**C**W**	**-E**R**L**Y**Q**Q**TLR**S	**AGK**	I**YMIFF**ML**VIFLGSFYLVNLILAVVAMAY**	416
$Na_v1.5$ II	**FH**A**FLI**I**FR**I**L**	**CGE-W**	**IETMWDCMEV**S	**GQ**S	L**CLLVF**LL**VMVIGNLVVLNLFLALLLSSF**	942
$Na_v1.5$ III	**GA**G**YL**A**LLQVA**	**TFKGW**	**-MDIMYAAVDS**	+	**YMY**I**YFVIFIIFGSFFTLNLFIGVIIDNF**	1473
$Na_v1.5$ IV	A**NS**ML**CLF**Q**IT**	**TSAGW**	**-DGLLSPILN**T	++	V**GILFF**TT**YIIISFLIVVNMYIA**I**ILENF**	1775

* : **R**NV**E**L**QP**KY**E**D**NL**

** : **GPP**D**CDP**DKDHPGSSVKR**DCG**N**P**S

: **R**EK**E**E**QP**HY**E**V**NL**

: **GPP**D**CDP**TLENPGTNVRG**DCG**N**P**S

+ : **R**GY**E**E**QP**QW**E**Y**NL**

++ : **GPP**Y**CDP**TLPNSNGS-RG**DCG**S**P**A

Figure 1

Molecular Pharmacology Fast Forward. Published on December 28, 2018 as DOI: 10.1124/mol.118.114025
This article has not been copyedited and formatted. The final version may differ from this version.

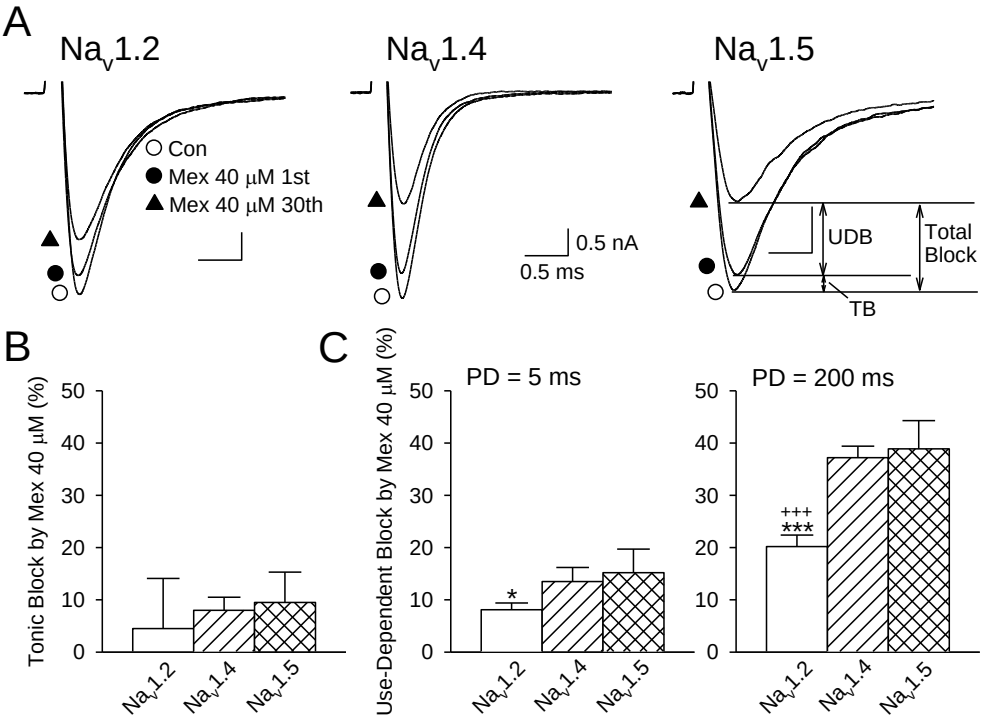

Figure 2

Molecular Pharmacology Fast Forward. Published on December 28, 2018 as DOI: 10.1124/mol.118.114025
This article has not been copyedited and formatted. The final version may differ from this version.

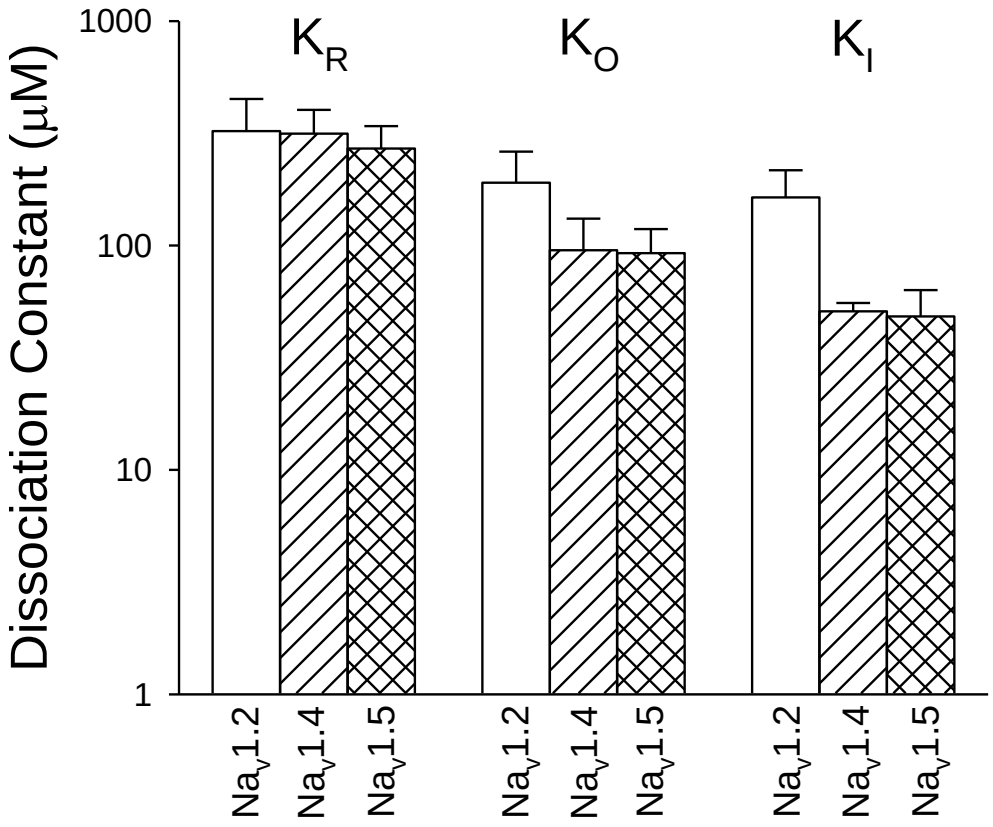

Figure 3

Molecular Pharmacology Fast Forward. Published on December 28, 2018 as DOI: 10.1124/mol.118.114025
This article has not been copyedited and formatted. The final version may differ from this version.

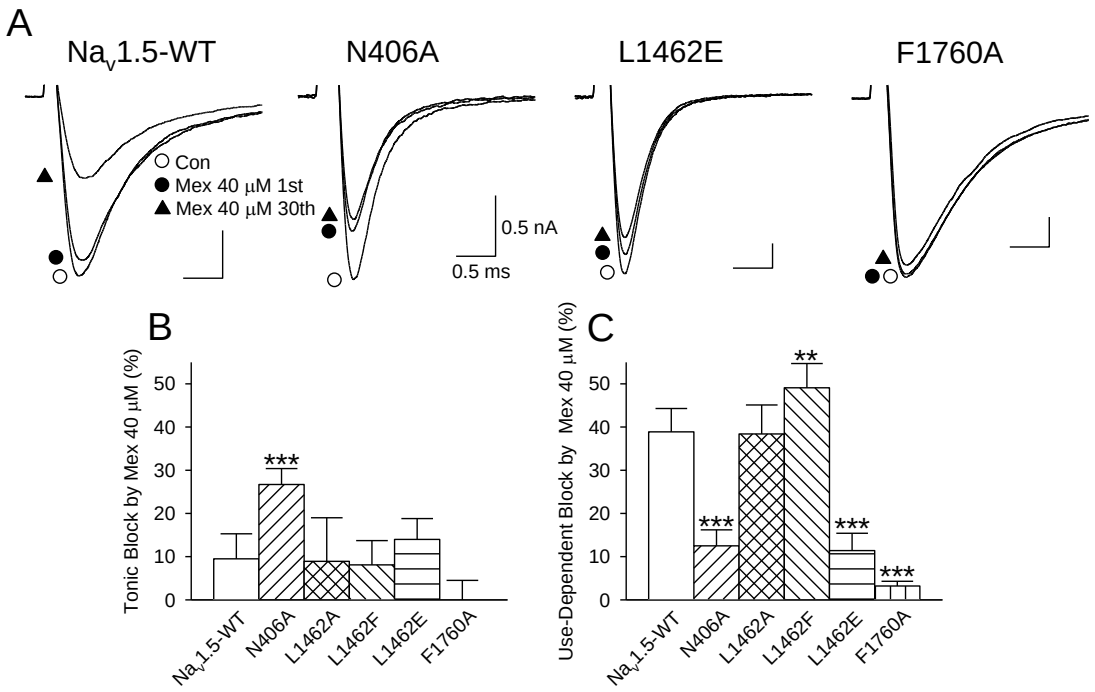

Figure 4

Molecular Pharmacology Fast Forward. Published on December 28, 2018 as DOI: 10.1124/mol.118.114025
This article has not been copyedited and formatted. The final version may differ from this version.

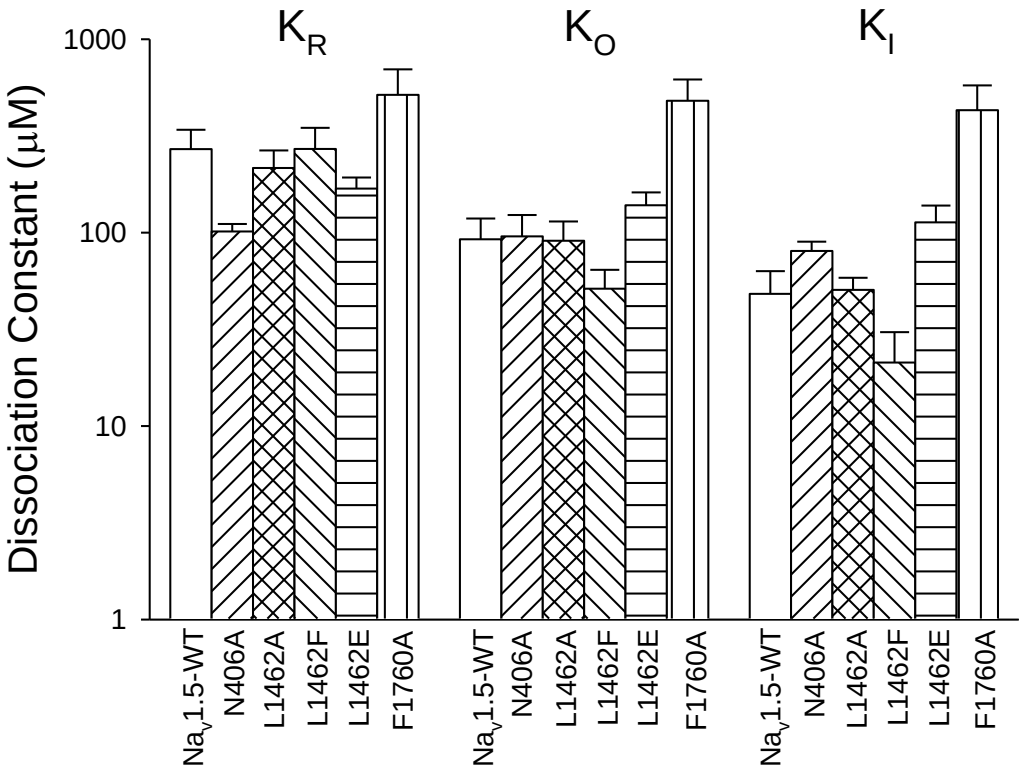

Figure 5

Molecular Pharmacology Fast Forward. Published on December 28, 2018 as DOI: 10.1124/mol.118.114025
This article has not been copyedited and formatted. The final version may differ from this version.

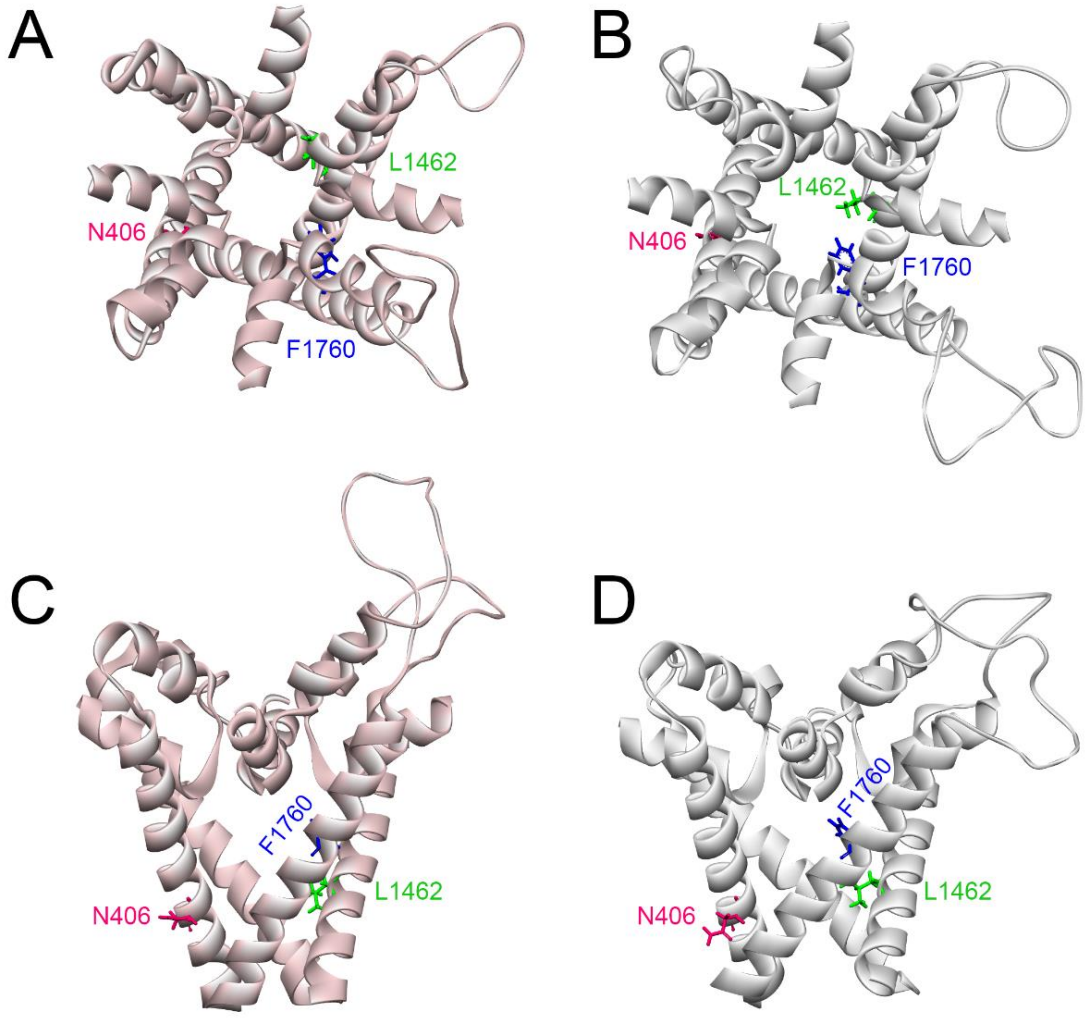

Figure 6

Molecular Pharmacology Fast Forward. Published on December 28, 2018 as DOI: 10.1124/mol.118.114025
This article has not been copyedited and formatted. The final version may differ from this version.

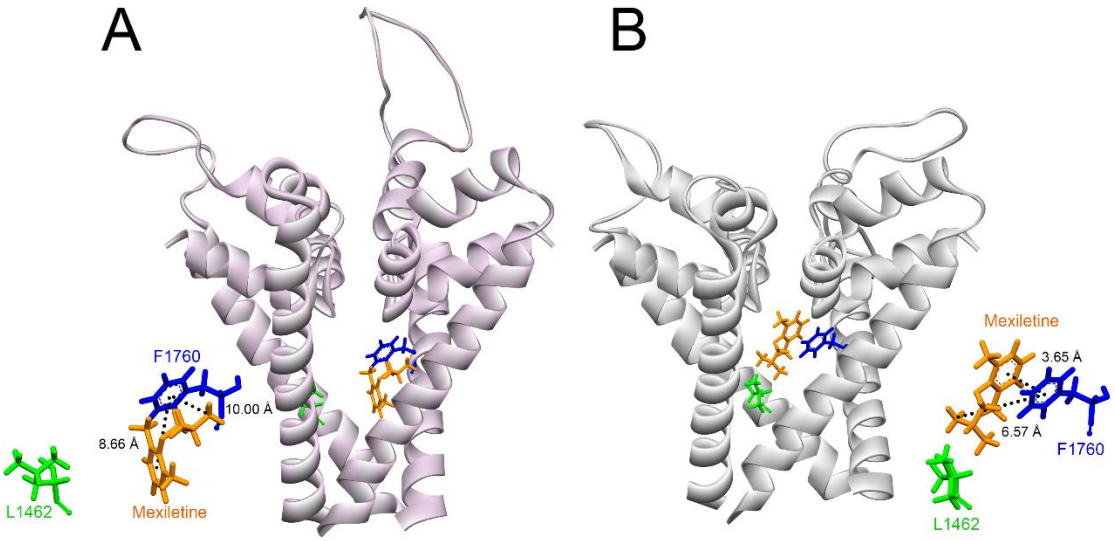

Figure 7

Molecular Pharmacology Fast Forward. Published on December 28, 2018 as DOI: 10.1124/mol.118.114025
This article has not been copyedited and formatted. The final version may differ from this version.

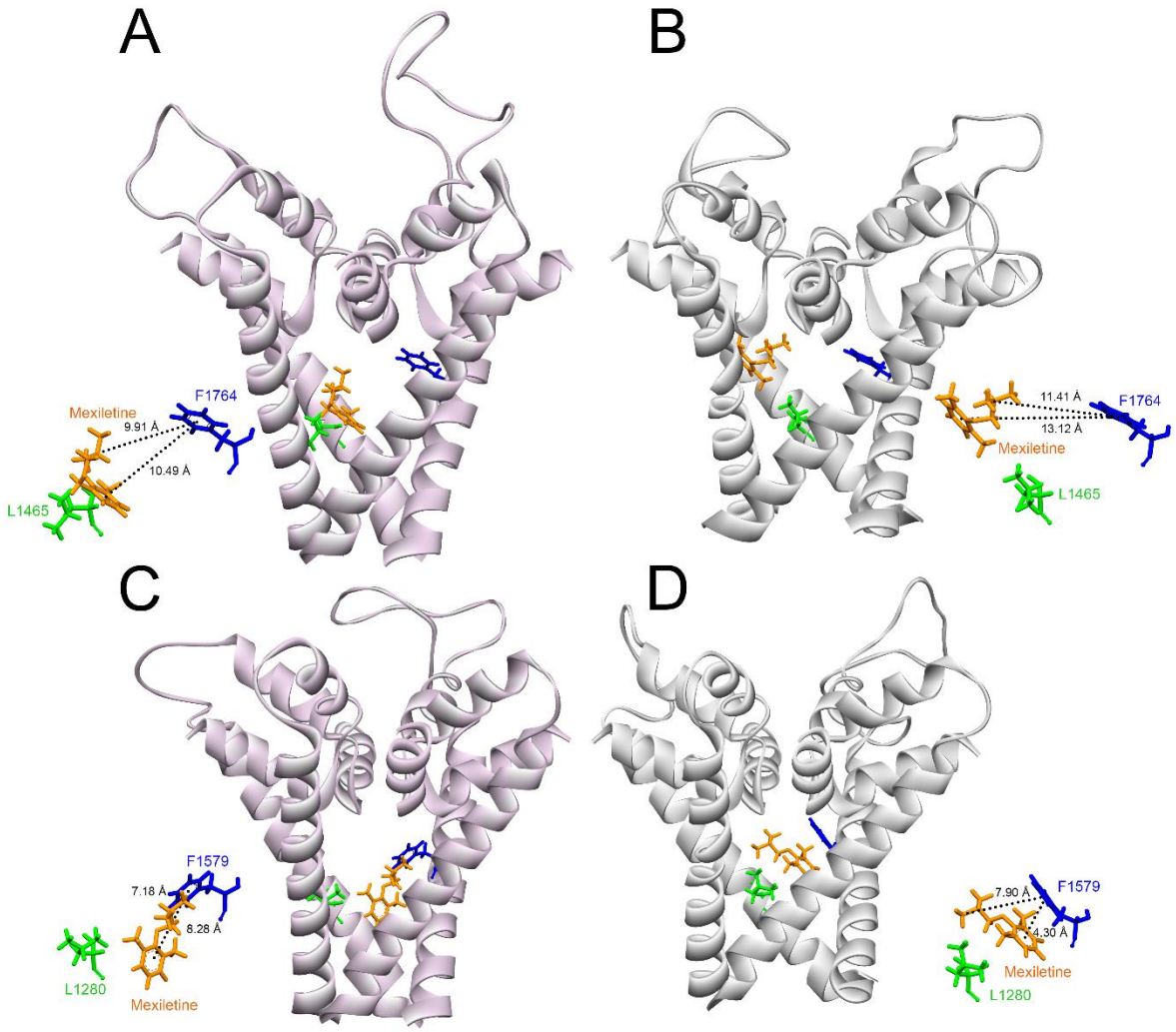

Figure 8

Molecular Pharmacology Fast Forward. Published on December 28, 2018 as DOI: 10.1124/mol.118.114025
This article has not been copyedited and formatted. The final version may differ from this version.

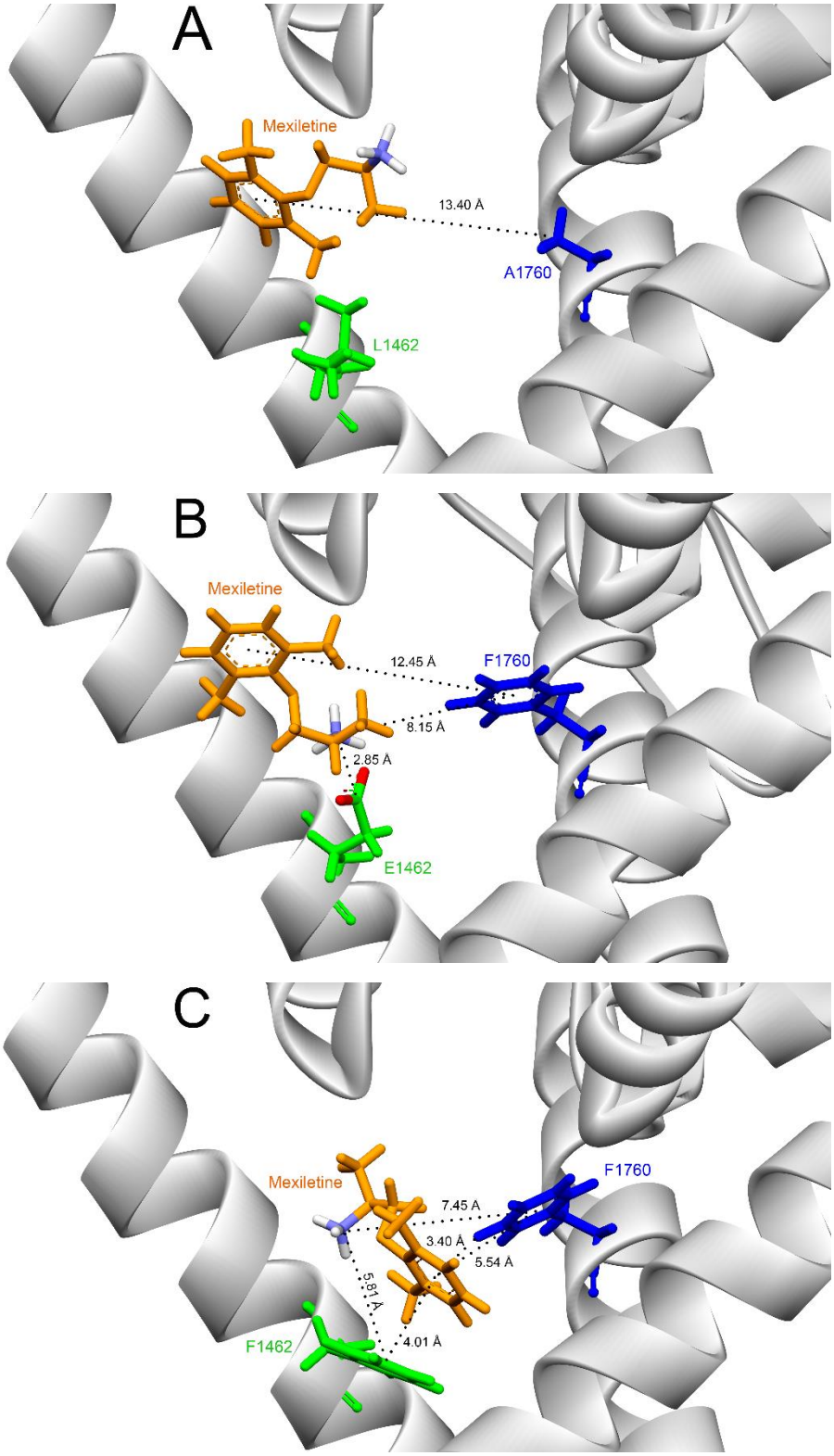

Figure 9